HHS Public Access

Author manuscript

Stat Med. Author manuscript; available in PMC 2017 July 20.

Published in final edited form as:

Stat Med. 2016 July 20; 35(16): 2786–2801. doi:10.1002/sim.6891.

Bayesian Multinomial Probit Modeling of Daily Windows of Susceptibility for Maternal $PM_{2.5}$ Exposure and Congenital Heart Defects

Joshua L. Warren[1], **Jeanette A. Stingone**[2], **Amy H. Herring**[3], **Thomas J. Luben**[4], **Montserrat Fuentes**[5], **Arthur S. Aylsworth**[6], **Peter H. Langlois**[7], **Lorenzo D. Botto**[8], **Adolfo Correa**[9], **Andrew F. Olshan**[10], and **the National Birth Defects Prevention Study**

[1]Department of Biostatistics, Yale School of Public Health, New Haven, Connecticut, USA

[2]Department of Preventive Medicine, Icahn School of Medicine at Mount Sinai, New York, New York, USA

[3]Department of Biostatistics, UNC Gillings School of Global Public Health, Chapel Hill, North Carolina, USA

[4]National Center for Environmental Assessment, Office of Research and Development, USA Environmental Protection Agency, Research Triangle Park, North Carolina, USA

[5]Department of Statistics, North Carolina State University, Raleigh, North Carolina, USA

[6]Departments of Pediatrics and Genetics, University of North Carolina at Chapel Hill, Chapel Hill, North Carolina, USA

[7]Texas Center for Birth Defects Research and Prevention, Texas Department of State Health Services, Austin, Texas, USA

[8]Division of Medical Genetics, Department of Pediatrics, University of Utah, Salt Lake City, Utah, USA

[9]Department of Pediatrics, University of Mississippi Medical Center, Jackson, Mississippi, USA

[10]Department of Epidemiology, UNC Gillings School of Global Public Health, Chapel Hill, North Carolina, USA

Abstract

Epidemiologic studies suggest maternal ambient air pollution exposure during critical periods of pregnancy is associated with adverse effects on fetal development. In this work, we introduce new methodology for identifying critical periods of development during post-conception gestational weeks 2–8 where elevated exposure to particulate matter less than 2.5 micrometers ($PM_{2.5}$) adversely impacts development of the heart. Past studies have focused on highly aggregated temporal levels of exposure during the pregnancy and have failed to account for anatomical

Corresponding Author: Joshua L. Warren, Department of Biostatistics, Yale School of Public Health, PO Box 208034 New Haven, CT 06520-8034. Phone: (203)785-4188. joshua.warren@yale.edu.

Supporting information:

Additional supporting information may be found in the online version of this article at the publisher's web site.

similarities between the considered congenital heart defects (CHDs). We introduce a multinomial probit model in the Bayesian setting that allows for joint identification of susceptible daily periods during pregnancy for 12 types of CHDs with respect to maternal $PM_{2.5}$ exposure. We apply the model to a dataset of mothers from the National Birth Defect Prevention Study where daily $PM_{2.5}$ exposures from post-conception gestational weeks 2–8 are assigned using predictions from the downscaler pollution model. This approach is compared to two aggregated exposure models that define exposure as the average value over post-conception gestational weeks 2–8 and the average over individual weeks respectively. Results suggest an association between increased $PM_{2.5}$ exposure on post-conception gestational day 53 with the development of pulmonary valve stenosis and exposures during days 50–51 with tetralogy of Fallot. Significant associations are masked when using the aggregated exposure models. Simulation study results suggest the findings are robust to multiple sources of error. The general form of the model allows for different exposures and health outcomes to be considered in future applications.

Keywords

Air pollution; Bayesian modeling; birth defects; critical windows; Gaussian process

Introduction

Congenital heart defects (CHDs), as a group, are the most common type of birth defect, with an estimated prevalence of 9 cases per 1,000 livebirths [1]. Previous research has sought to determine if CHDs are associated with exposure to fine particulate matter less than 2.5 micrometers in diameter ($PM_{2.5}$) during gestation [2–7]. Evidence of a relationship has been inconsistent across studies, potentially due to differences in how studies classify CHD cases and measure/define exposure. CHDs include a causally heterogeneous group of morphologic anomalies involving potentially numerous developmental pathways and pathogenetic mechanisms. Multiple classification and aggregation schemes exist to ensure consistency for varying surveillance and research purposes, as well as to address issues of small sample size of individual defects through aggregation into broader defect-grouping categories. The use of overly aggregated or incorrect groupings as outcomes in epidemiologic studies, however, may bias effect estimates, potentially masking relevant etiologic relationships [8].

Failing to account for exposure timing may also mask associations. Typical cardiac development involves a coordinated series of precise steps, beginning with the migration of cells to form the endocardial tubes and culminating in the eighth week post-conception with the septation of the ventricles and outflow tracts [9]. Insults in early parts of this window of cardiac development may have different effects on development and ultimate cardiac anatomy than those toward the end of the window when the structures are almost completely formed. This concept is supported by previous work that examined maternal exposure to $PM_{2.5}$ and CHDs, finding that some associations were obscured when exposure over the entire window of cardiac development was averaged, instead of simultaneously examining individual weeks of exposure during post-conception weeks 2–8 [5].

Similar findings of variability within the window of cardiac development were reported in a recent study [10]. In that study, a novel model utilizing a Bayesian hierarchical framework was developed to investigate potential windows of vulnerability to air pollutants using weekly averages during cardiac development. The model improved estimation of critical windows by allowing for non-Gaussian and nonstationary spatial-temporal pollution associations, resulting in increased modeling flexibility. Using weekly averages, however, limited the number of exposure data points and the model's ability to estimate more precise windows during the period of cardiac development.

In this paper, we introduce new methodology in the Bayesian setting to explore a finer temporal resolution of pollutant exposure by including daily as opposed to weekly averages. Exploring daily averages should provide more detailed insight into critical pregnancy periods that may be overlooked when higher levels of aggregation are considered, particularly for congenital heart defects for which the exposure period of interest is relatively short. The newly developed model is also able to jointly analyze windows of susceptibility for 12 types of CHDs while allowing for potential similarities in the windows across the broader defect-groupings created from a detailed defect classification scheme. Accounting for these shared characteristics within defect-groupings could improve both estimation and precision of the critical periods for individual defects. The previous study [10] included only three types of CHDs and did not incorporate the broader defect-groupings information into the modeling. We also extend the previous work by allowing for multinomial responses as opposed to conditionally independent binary responses.

This analysis was carried out using data from the National Birth Defects Prevention Study (NBDPS), a national population-based case-control study of birth defects, and $PM_{2.5}$ exposure estimates from the Environmental Protection Agency's (EPA) downscaler Community Multiscale Air Quality (CMAQ) model, a spatiotemporal pollutant model that provides daily estimates of $PM_{2.5}$ by combining numerical output from the CMAQ chemical model with available ambient monitoring data [11].

While our application of the introduced methodology is focused on daily air pollution exposure and CHD development, we note that the general formulation of the model allows for any type of time-varying exposure and multivariate health outcome of interest. Example exposures include pesticides, contaminated drinking water, pollen, secondhand smoke, and other air pollutants. Alternative reproductive health outcomes such as preterm birth and low birth weight could be considered as well as more general acute responses including allergic reactions, respiratory events, and cardiovascular events. Use of finer levels of temporal aggregation for the exposure is also possible, if appropriate, as is the number of categories of the health response. Introducing the model for multinomial responses will also allow for critical window identification in data settings where the assumption of conditionally independent binary responses may be inappropriate.

In Section 2, we describe the data used in the study. The general form of the statistical model is presented in Section 3 and we apply the model to our data in Section 4. A simulation study is presented in Section 5 to assess the robustness of our findings to different sources of misclassification error. We close in Section 6 with discussion.

Data description

Study population

We utilize data from the NBDPS from years 2001–2006. The methods of the NBDPS have been described previously [12]. Cases are livebirths, stillbirths greater than 20 weeks gestation or at least 500 grams, and elective terminations where available, that were identified by the birth defects monitoring programs in nine sites within the United States (US) (Arkansas, metropolitan Atlanta, California, Iowa, Massachusetts, New York, North Carolina, Texas, Utah). A tenth site, New Jersey, was not included in our analysis as geocoded residential information was unavailable. Cases with CHDs of known cause, such as chromosome abnormalities and single gene syndromes, were excluded per NBDPS protocol. Controls are livebirths without any known birth defects, identified through vital or hospital records, depending upon site-specific protocols. We limit our population to women who lived in geographic locations where downscaler CMAQ predictions were available during the study period. This led to the exclusion of women from the California and Utah study centers and women from the Texas center who conceived in 2001. Case homogeneity is an important component in understanding human teratogenesis [8,13] and can potentially improve risk estimation [14] in epidemiologic studies. In order to create homogeneous case groups and avoid confusing causes related to single versus multiple defects, we included cases with only a single CHD and no major, reportable extra-cardiac defects present. We also exclude women who had pregestational diabetes because of the established strong association with CHDs in offspring [15]. Women with missing covariate information are also excluded ($n = 78$), resulting in a total sample size of 4,727. See Table 1 for a breakdown of sample size by specific CHD.

As part of the NBDPS protocol, medical records of CHD cases were reviewed by a team of clinicians with training in pediatric cardiology using standardized protocols and assigned a single individual defect and a corresponding broader defect-grouping based on anatomical and developmental considerations [8]. The six broader defect-groupings included in this analysis, along with the individual defects that comprise them are as follows:

1. Left ventricular outflow tract obstructions (LVOTO) including
   - coarctation of the aorta (COA),
   - hypoplastic left heart syndrome (HLHS), and
   - aortic stenosis (AS);
2. Right ventricular outflow tract obstructions (RVOTO) including
   - pulmonary valve stenosis (PVS) and
   - atresia (pulmonary and tricuspid atresia);
3. Conotruncal defects including
   - dextro-transposition of the great arteries (d-TGA),
   - tetralogy of Fallot (TOF), and

- other conotruncal defects (OC) (common truncus, interrupted aortic arch-type B and type not otherwise specified, double outlet right ventricle whether or not associated with transposition of the great arteries, and conoventricular septal defects);

4. Septal defects including
   - atrial septal defects (ASD) and
   - perimembranous ventricular septal defects (VSDpm);
5. Atrioventricular septal defect (AVSD); and
6. Anomalous pulmonary venous return (APVR) (includes total APVR and partial APVR).

Exposure assignment

As part of the NBDPS protocol, women reported their complete residential history during pregnancy. All maternal residences were geocoded centrally by the Agency for Toxic Substances and Disease Registry to maintain consistency between study sites. We use each woman's geocoded address for the first eight weeks of pregnancy (post-conception) to assign exposure. Per NBDPS protocol, each woman's estimated date of conception is calculated using the estimated date of delivery, that is, the due date that the woman received from her physician and reported during the study interview. That estimated date of conception is used to assign daily exposures for gestational weeks 2–8. For women who had more than one address during that period, each address is used to assign exposure during the time the woman resided at that location. Exposure is calculated using output from EPA's downscaler CMAQ model. Described previously [11], this model scales gridded CMAQ output down to point-level monitoring data and combines the two using linear regression with spatially- and temporally-varying bias coefficients. It provides bias-corrected, daily point predictions of 24-hour $PM_{2.5}$ at the centroid of each census-tract in the US. Previous research using the ozone estimates from this exposure model suggests that results obtained when using the downscaler CMAQ model are similar to those obtained when using monitoring data but have greater precision due to the inclusion of populations that do not have available monitoring data [16]. We compile exposure data for the entire eastern US for the years 2001–2006. Each woman is matched to the closest census-tract centroid, and we then obtain daily averages for post-conception gestational weeks 2 through 8 to correspond with the critical period of cardiac development. For numerical stability during model fitting, each gestational day average exposure is standardized across all women to have a mean of zero and standard deviation of one.

Methods

Statistical model

We model the multinomial vector of possible CHD outcomes from each birth using a multinomial probit regression model such that $\boldsymbol{Y}_i|\boldsymbol{p}_i \overset{\text{ind}}{\sim} \text{Multinomial}(1;\boldsymbol{p}_i)$ where $\boldsymbol{p}_i = (p_{i1}, \ldots, p_{iJ}, p_{ic})^T$, p_{ij} is the probability that birth i results in CHD j, p_{ic} is the probability that birth

i does not result in one of the included CHDs (control), and *J* is the number of CHDs considered in the study. In our application, $J = 12$, but in general $J \geq 1$. $\mathbf{Y}_i = (Y_{i1}, \ldots, Y_{iJ}, Y_{ic})^T$ where $Y_{ij} = 1$ and $Y_{ik} = 0$, $k \neq j$ when birth *i* results in CHD *j*. We work with multinomial responses of size one since each birth can only result in a single CHD or control outcome such that $\sum_{j=1}^{J} Y_{ij} + Y_{ic} = 1$ for all *i*. We require the set of probabilities for each birth to sum to one in order to have a valid model and note that these probabilities do not represent prevalences due to the case-control design of the study. As a result, the multinomial probit model is most naturally introduced through the use of latent variables which are jointly defined and lead to the satisfaction of this requirement. Previous research showed that in the Bayesian setting, the prospective logistic regression model inference is equivalent to the corresponding retrospective inference under certain assumptions regarding the prior distribution of the log odds for a diseased individual with baseline exposure and for the prior distribution of exposure probabilities for the control group [17]. This result suggests that the Bayesian analysis of case-control studies may be carried out using a prospective model, similar to the frequentist setting.

For woman *i*, we introduce the set of latent variables $\mathbf{w}_i = (w_{i1}, \ldots, w_{iJ})^T$ such that

$$w_{ij} = \mathbf{x}_i^T \boldsymbol{\beta}_j + \sum_{k=k_0}^{K} z\{\boldsymbol{s}_i, t(k)_i\} \eta_{g(j)}(j,k) + \varepsilon_{ij}$$

where $\mathbf{x}_i$ is a vector of potential confounders and individual-level covariates, $\boldsymbol{\beta}_j$ is the vector of regression coefficients specific to CHD *j* that relates the covariates to the latent response, $z\{\boldsymbol{s}_i, t(k)_i\}$ is the k^{th} post-conception gestational day average of downscaled $PM_{2.5}$ exposure (standardized at each gestational day across all women) at the census tract centroid closest to maternal residence location $\boldsymbol{s}_i$ during calendar period $t(k)_i$, $\eta_{g(j)}(j, k)$ is the pollution parameter specific to post-conception gestational day *k* and defect *j* belonging to broader defect-grouping $g(j)$, and $\varepsilon_{ij} \overset{\text{iid}}{\sim} N(0,1)$. Specifying $\varepsilon_{ij} \overset{\text{iid}}{\sim} N(0,1)$ ensures that the introduced regression parameters and daily risk parameters are well identified [18]. The $t(k)_i$ function maps an input gestational day to the appropriate calendar date of gestation for woman *i* since women in the study were pregnant during different calendar periods. Because we are interested in daily exposures during post-conception gestational weeks 2–8, we select $k_0 = 8$ and $K = 56$ in our application of the model.

The latent variables are used to directly define the observed outcomes such that $Y_{ik} = 1$ (CHD *k* is observed) if $\max\{\mathbf{w}_i\} = w_{ik} > 0$ and $Y_{ic} = 1$ (control is observed) if $\max\{\mathbf{w}_i\} < 0$. This leads to $p_{ik} = P(\max\{\mathbf{w}_i\} = w_{ik} > 0)$ for $k = 1, \ldots, J$ and $p_{ic} = P(\max\{\mathbf{w}_i\} = w_{ik} < 0)$, where $P(A)$ represents the probability of event *A* occurring. Therefore, increasing the value of the latent variable associated with a particular CHD directly increases the probability that the respective outcome is observed. Identifying factors that significantly increase/decrease the latent responses provides insight into the associations with the respective CHDs.

The general form of the model allows for the possibility that the included confounders are associated with each CHD differently through the use of CHD-specific parameter vectors $\boldsymbol{\beta}_j$,

$j = 1, \ldots, J$. Based on directed acyclic graph analysis, all models are adjusted for the following confounders: maternal age as a continuous variable; maternal race/ethnicity using self-reported categories of White non-Latina, Black non-Latina, or other; maternal education categorized as less than high school, high school diploma/equivalency and/or some college or trade school, and college graduate or advanced degree; maternal tobacco use during the first month of pregnancy categorized dichotomously as any/none; and maternal alcohol consumption during the first three months of pregnancy categorized dichotomously as any/none. Maternal age was coded as a single, continuous variable as previous research has shown that the prevalence of isolated CHDs increases with greater maternal age [19]. Models are also adjusted for each center's ratio of septal defects to total CHDs in order to account for potential differences in case ascertainment by study center because identifying septal defects is often dependent upon the method of case ascertainment [20].

In order to identify daily critical windows of importance for each CHD, we allow for daily and CHD-specific pollution parameters in the model formulation through use of $\eta_{g(j)}(j, k)$. These parameters capture the association between the average amount of pollution exposure during post-conception gestational day k and CHD j within broader defect-grouping $g(j)$. In total, we introduce J sets of these parameters, $\boldsymbol{\eta}_{g(j)}(j)$, $j = 1, \ldots, J$, one for each CHD such that $\boldsymbol{\eta}_{g(j)}(j) = \{\eta_{g(j)}(j, k_0), \ldots, \eta_{g(j)}(j, K)\}^T$. Using the six previously established broader defect-groupings, we are able to place each individual CHD into a larger, anatomically-based defect category such that $g(j) \in \{1, \ldots, G\}$ for all j where $G = 6$ in our application. These groupings, given in the Study Population Subsection, allow us to introduce prior distributions for the model parameters that account for the possibility that associations between $PM_{2.5}$ exposure and CHD development are similar within a broader grouping. We also allow for the possibility that the daily associations within a single CHD are similar due to proximity in time. Adding this temporal correlation structure also helps to account for the multicollinearity introduced by using a finer time scale as exposures closer in time are likely highly correlated.

Prior information/induced covariance

The model specification is completed by assigning prior distributions to the introduced model parameters. Use of the multinomial probit model results in semi-conjugacy and therefore allows for more efficient estimation of the introduced parameters. The vectors of pollution parameters within a single broader CHD grouping are modeled jointly and assigned a multivariate normal prior distribution which allows for temporal correlation between the daily association parameters and a cross-covariance between the parameters of the included CHDs. For example, for broader CHD grouping 1 ($g(j) = 1$) we specify a prior distribution for $\{\boldsymbol{\eta}_1(1)^T, \boldsymbol{\eta}_1(2)^T, \boldsymbol{\eta}_1(3)^T\}^T$ while for grouping 2 we assign an independent prior distribution to $\{\boldsymbol{\eta}_2(4)^T, \boldsymbol{\eta}_2(5)^T\}^T$. We refer to these group-specific vectors as $\boldsymbol{\eta}^{(g)}$, for $g \in \{1, \ldots, G\}$. The selected prior distributions are given as

$\boldsymbol{\eta}^{(g)} | \phi_g, \Omega^{(g)} \overset{\text{ind}}{\sim} \text{MVN}\{\mathbf{0}, \Omega^{(g)} \otimes \Sigma(\phi_g)\}$ where $\otimes$ represents the Kronecker product and $\Omega^{(g)}$ is the cross-covariance matrix for broader grouping g. This n_g by n_g matrix describes the covariance between association parameters from the individual CHDs within the same broader grouping where n_g is the number of CHDs in broader grouping g. We assume a very general structure for this covariance, allowing for all possible levels of correlation (positive

and negative) between each of the daily association parameters connected with different CHDs. This is achieved by assigning independent inverse Wishart prior distributions to $\Omega^{(g)}$ with scale matrix equal to the n_g by n_g identity matrix and degrees of freedom equal to n_g. These vague yet proper prior distributions allow the data to drive the resulting inference.

Within a single CHD, we allow for the possibility that association parameters closer in time are more highly correlated through the use of $\Sigma(\varphi_g)$. The entries of $\Sigma(\varphi_g)$ are given as $\Sigma(\varphi_g)_{k,k'} = \text{Corr}\{\eta_g(j, k), \eta_g(j, k')\} = \exp\{-\varphi_g|k - k'|\}$ where $\varphi_g > 0$ is the parameter specific to broader grouping g that controls the level of temporal correlation between the association parameters. Large values of φ_g suggest that association parameters close in time are not highly correlated while small values suggest the opposite. We allow for this parameter to vary based on the grouping for increased flexibility and generality. As the number of days increases between two parameters, the correlation decreases. This introduced prior distribution leads to a general covariance structure between the association parameters such that

$$\text{Cov}\{\eta_{g(j)}(j,k), \eta_{g(j')}(j',k')\} = \begin{cases} \Omega^{(g)}_{j,j'} \exp\{-\phi_g|k-k'|\}, & \text{if } g(j) = g(j') \equiv g \\ 0, & \text{otherwise.} \end{cases}$$

This structure encourages sharing of information not only across pregnancy days but also across the individual defects within a broader CHD grouping. However, if this sharing of information is not warranted, the model allows for that possibility as well.

The parameters that control the level of temporal correlation are given independent uniform prior distributions such that $\phi_g \overset{\text{iid}}{\sim} \text{Uniform}(a, b)$. These parameters and the cross-covariance parameters are well identified given the identifiability of the daily risk parameters. The values of a and b are chosen so that the prior correlation between the daily association parameters from any two time periods is allowed to vary between 0.001 and 0.999. This allows the amount of smoothness exhibited between the association parameters to be determined by the data rather than an informative prior distribution. Using the prior correlation function between the daily risk parameters from the same defect, $\text{Corr}\{\eta_g(j, k), \eta_g(j, k')\} = \exp\{-\varphi_g|k - k'|\}$, we found the value of φ_g such that $\exp\{-\varphi_g|k - k'|\} = 0.001$ when $|k - k'| = 1$ (smallest difference between two different daily parameters). Solving for φ_g, we obtain the upper bound $b = 6.9$. For the lower limit of the uniform prior, we found the value of φ_g such that $\exp\{-\varphi_g|k - k'|\} = 0.999$ when $|k - k'| = 48$ (largest difference between two different daily parameters). Solving for φ_g, we obtain the lower bound $a = 2.1 * 10^{-5}$. The regression parameters associated with the individual-level covariates are given independent and identically distributed prior distributions such that $\beta_{jk} \overset{\text{iid}}{\sim} \text{N}(0, \sigma^2_\beta)$ where σ^2_β is fixed at a large value (10^{10}), resulting in vague yet proper prior distributions for these parameters.

Data application

We apply the introduced model to the combined NBDPS and downscaler $PM_{2.5}$ exposure dataset. All results are based on a total of 280,000 samples from the posterior distribution of

the model parameters (140,000 samples each from two chains with different starting values) after a burn-in period of 10,000 iterations for each chain. All models were fit using R statistical software [21] and the model fitting details are provided in Appendix A. Batch mean Monte Carlo (MC) standard errors [22] were calculated for all presented posterior means in order to determine the appropriate number of posterior samples to obtain during the MCMC sampling. The MC standard errors for the daily association parameters presented in Figures 1–3 and Supplemental Material, Figure S6–Figure S8 range from 0.00002 to 0.00026 with a median value of 0.00005. Convergence was determined based on visual inspection of the trace plots from all model parameters as well as the calculation of Gelman and Rubin's convergence diagnostic, the potential scale reduction factor, for each model parameter [23–24]. The average, median, minimum, and maximum values for the estimated potential scale reduction factor across all parameters was 1.00, 1.00, 1.00, and 1.06 respectively. Recall that large values of this metric for a parameter indicate nonconvergence and values near one indicate that each chain has reached its target distribution. Boxplots of the effective sample sizes for each group of model parameters are displayed in Supplemental Material, Figure S1. The effective sample sizes ranged from 1,445 to 89,084 across all parameters. Supplemental Material, Figure S2 displays trace plots for selected daily association parameters, $\eta_{g(j)}(j, k)$, one from each defect. For PVS and TOF, days 53 and 51 respectively are displayed since these are identified as having 95% credible intervals (CIs) that do not include zero. For the remaining defects, the day was chosen at random. These presented plots are typical of other daily association parameter trace plots. Supplemental Material, Figures S3–S4 show additional trace plots for all φ_g parameters and for all diagonal elements of each $\Omega^{(g)}$ matrix, respectively. Posterior means and posterior standard deviations are also presented.

The main parameters of interest, $\eta_{g(j)}(j, k)$, capture the association between the average amount of pollution exposure during post-conception gestational day k and CHD j within broader defect-grouping $g(j)$. Because the $PM_{2.5}$ exposure at each gestational day is standardized across all women, the interpretation of a single parameter is that a one standard deviation increase of average $PM_{2.5}$ exposure during post-conception gestational day k increases the probability of developing CHD j by increasing the respective latent variable by $\eta_{g(j)}(j, k)$. Supplemental Material, Figure S5 displays the mean and standard deviation of $PM_{2.5}$ exposures averaged across all women for each post-conception gestational day.

Table 1 displays the characteristics of our study population by specific CHD/control status. Figures 1–3 and Supplemental Material, Figure S6–Figure S8 display graphical results from the newly introduced model that describes the association between $PM_{2.5}$ exposure during specific cardiac development days and the development of each included CHD. Each figure represents a broader CHD grouping. For each daily exposure window during post-conception gestational weeks 2–8, posterior means and 95% CIs are plotted.

Based on these results, we now have increased insight regarding $PM_{2.5}$'s impact on CHD development during specific periods of pregnancy. Recall that an increase in the latent variable directly increases the probability that the respective CHD is observed since the maximum latent variable (larger than zero) for an individual defines the outcome such that $Y_{ik} = 1$ if $\max\{\boldsymbol{w}_i\} = w_{ik} > 0$. In particular, in the RVOTO grouping, PVS (Figure 1A) is

shown to be positively associated with $PM_{2.5}$ exposure experienced during the end of week 8 of pregnancy (post-conception gestational day 53). This suggests that an increase of 6.51 micrograms per cubic meter (μg/m^3) (1 standard deviation) of average $PM_{2.5}$ exposure during post-conception gestational day 53 significantly increases the probability of developing PVS by increasing the respective latent variable by 0.0178 (95% CI 0.0011, 0.0374). For reference, the average daily exposure for the included women across all days was 12.30 μg/m^3. Also, in the conotruncals grouping, TOF (Figure 2B) is shown to be positively associated with $PM_{2.5}$ exposure during the early part of pregnancy week 8 (post-conception gestational days 50–51). This suggests that an increase of 6.44 and 6.46 μg/m^3 of average $PM_{2.5}$ exposure during post-conception gestational days 50 and 51 respectively, significantly increases the probability of developing TOF by increasing the respective latent variable by 0.0154 (95% CI 0.0001, 0.0330) and 0.0159 (95% CI 0.0005, 0.0336). The largest estimated association parameter is observed for AVSD (Figure 3) at post-conception gestational day fourteen. A 6.47 μg/m^3 increase in $PM_{2.5}$ exposure during this day leads to an increase in the latent variable of 0.0239 (95% CI −0.0052, 0.0657). The 95% CI for this parameter includes zero largely due to the small sample size observed for the AVSD outcome (38 cases). This is the smallest sample size of any CHD included in the analysis. The results also suggest that averaging $PM_{2.5}$ exposure over weeks 2–8 may be less informative since a majority of the timeframe results in a null association for each of the defects. Susceptible windows of importance may be missed due to averaging in this way.

The cross-covariance results within each broader defect-grouping suggest that the individual CHDs generally have little correlation in terms of the association with $PM_{2.5}$ exposure. For the LVOTO grouping, the median posterior correlation (and posterior standard deviation) between COA and HLHS is 0.041 (0.351), between COA and AS is 0.046 (0.381), and between HLHS and AS is 0.025 (0.393). For the RVOTO grouping, the correlation between PVS and atresia is 0.073 (0.381). The highest correlation is estimated in the conotruncal grouping, where the correlation between d-TGA and OC is 0.123 (0.379), between d-TGA and TOF is −0.011 (0.364), and between TOF and OC is −0.060 (0.372). The correlation between ASD and VSDpm of the septal group is −0.011 (0.361). While posterior correlations between daily risk parameters from different CHDs within the same major grouping are low, the correlation between daily risk parameters from the same CHD are close to one even for large daily differences ($|k - k'|$). Similar levels of temporal correlation were observed in previous susceptible window research [16,25].

Model comparisons

In order to explore the impact of considering daily pollution exposure averages across the entire post-conception gestational weeks 2–8, we also fit a standard pollution exposure and CHD development model (Model 2) and a model with weekly pollution exposure averages (Model 3). For Model 2, we once again assume a multinomial probit model form as in the newly introduced model (Model 1). However, instead of introducing separate daily pollution exposure parameters as in Model 1, we only include the complete weeks 2–8 pollution average as a single predictor. The latent variables are defined as $w_{ij} = \mathbf{x}_i^T \boldsymbol{\beta}_j + \bar{z}_{t_i}(\boldsymbol{s}_i)\theta_j + \varepsilon_{ij}$ where $\bar{z}_{t_i}(\boldsymbol{s}_i) = \frac{1}{49}\sum_{k=8}^{56} z\{\boldsymbol{s}_i, t(k)_i\}$ represents the week 2–8 $PM_{2.5}$ average at the census

tract centroid closest to location s_i during calendar period $t(8)_i, \ldots, t(56)_i$ specific to woman i's dates of pregnancy. θ_j represents the pollution association parameter associated with CHD j. Model 3 has similar likelihood form and prior specifications as Model 1 but uses weekly pollution exposure averages (weeks 2–8) instead of daily averages. Models 2–3 are also fit in the Bayesian setting to allow for direct comparison with Model 1.

The posterior inference from Model 2 for the pollution parameters (θ_j) is shown in Table 2. None of the CHD-specific parameter estimates are significantly associated with an increase/decrease in the likelihood of developing any of the considered CHDs. The results observed using Model 1 are missed when an aggregated pollution exposure is used instead.

The posterior inference from Model 3 is shown in Supplemental Material, Figures S9–S14. The weekly model results suggest only a single critical window during the pregnancy for any of the defects. This window is seen for pulmonary valve stenosis during post-conception gestational week 8 where the weekly risk parameter has a posterior mean estimate of 0.068 (95% CI 0.003, 0.143). This finding is in agreement with our results from Model 1 where day 53 during week 8 was identified. However, we have gained precision in estimating these critical windows and it appears that the weekly findings are being driven mainly by the increased risk seen around day 53. The major benefit of considering daily exposures is seen more clearly for the TOF results. In Model 1, we identified days 50–51 as being associated with elevated risk due to increased pollution exposure. However, Model 3 is unable to detect this effect likely due to averaging over the daily risks. In Figure 2, it is clear that days 52–56 do not have a clear signal and indicate no association with increased risk. Model 3 averages over these days and as a result, doesn't have the flexibility to identify week 8 as being a potential critical window, as the 95% CI now includes zero. Therefore, Model 1 is necessary in this setting to properly identify critical windows during the pregnancy.

We formally compare the fits from each model using a previously developed posterior predictive model selection technique [26]. Briefly, replicate responses are simulated from the posterior predictive distribution (ppd) and a discrepancy function is selected that describes the difference between the observed responses and those simulated from the ppd. The posterior expectation of the discrepancy metric is estimated using the MCMC posterior samples and this value is compared among values from competing models. The model with the smallest value is then selected. For non-Gaussian response data, the deviance criterion of the likelihood is most often selected as the discrepancy function. Values of this comparison metric are estimated to be 6,178.60 (Model 1), 6,185.19 (Model 2), and 6,184.09 (Model 3) suggesting that Model 1 may be preferred in terms of posterior predictive model fit. Overall, Model 1 appears to provide adequate fit to the data, similar to less complex competing models, but is also able to identify critical windows that are not seen using the other approaches.

Simulation study

Use of this model requires the ability to assign exposure amounts to each individual during a selected timeframe before the health outcome is observed. Often, these exposures and the exposure timing are measured with error. We conduct a simulation study in order to

determine the impact of uncertainty in gestational age and pollution exposure estimates on the resulting model inference. We hypothesize that because this uncertainty affects both cases and controls similarly, the daily association parameter estimates will be closer to zero, indicating a null association.

We begin by creating a true set of gestational ages and pollution exposures for a population of interest. In order to resemble a realistic and therefore meaningful scenario, we use our NBDPS sample of births directly and assume that the gestational ages and pollution exposures are observed without error. Under this assumption, we then run a reduced version of the introduced model for a single defect. We choose to work with TOF due to the signal observed during post-conception gestational days 50 and 51 (Figure 2B).

After fitting the model, we obtain the estimated daily association parameters and 95% CIs as displayed using the black plotting symbols in each panel of Figure 4. As with the original findings, post-conception gestational days 50 and 51 are identified as having 95% CIs that do not include zero. In the simulation study, these results are treated as the true model inference of interest because we are assuming that gestational age and pollution exposures are observed without error. However, in practice we are unable to precisely determine the exact personal exposure amount and gestational age for each woman. In order to account for this uncertainty, we add error to the true gestational ages and pollution exposures and refit the model to estimate the daily association parameters. If the introduced errors have little impact on the critical window estimation, we would expect to see (i) similar temporal trends in the daily association parameter estimates/CIs and (ii) similar identification of statistically significant estimates, when compared to the true (error-free) model inference.

We consider three levels of error each for gestational age and pollution exposure. For gestational age, we add an independent, normally distributed error centered at zero with variance σ^2_{ga} to each individual's gestational age. We then round this new gestational age estimate to the nearest day to resemble our observed data. For small, medium, and large errors we select $\sigma^2_{ga}=0.50$, $\sigma^2_{ga}=2.30$, and $\sigma^2_{ga}=8.50$, respectively. These settings correspond to a maximum observed difference between true and displaced gestational age of 3, 7, and 14 days, respectively.

For the daily pollution exposures, we add independent, normally distributed random errors centered at zero with variance σ^2_p to each daily pollution amount. In order to ensure that negative and/or unrealistically large values of exposure are not created, we require that each displaced exposure lies between 0 and the largest observed exposure amount by using the truncated normal distribution to simulate errors. For small, medium, and large errors we select $\sigma^2_p=7.84$, $\sigma^2_p=43.56$, and $\sigma^2_p=1296.00$, respectively. These settings correspond to an observed average correlation between true and displaced pollution exposures across individuals of 0.83, 0.54, and 0.09, respectively. These values are selected based on the reported correlations in a number of studies investigating the agreement between personal and ambient $PM_{2.5}$ exposures [27]. Displaced daily pollution exposures were then standardized as previously described.

For each setting of the gestational age and pollution exposure errors, we create 100 datasets for analysis. This process replicates what is typically done in practice, with the difference being we now know the true values associated with the estimates. In total, we consider nine settings such that:

- Error Setting 1: Large gestational age error, large pollution exposure error;
- Error Setting 2: Large gestational age error, medium pollution exposure error;
- Error Setting 3: Large gestational age error, small pollution exposure error;
- Error Setting 4: Medium gestational age error, large pollution exposure error;
- Error Setting 5: Medium gestational age error, medium pollution exposure error;
- Error Setting 6: Medium gestational age error, small pollution exposure error;
- Error Setting 7: Small gestational age error, large pollution exposure error;
- Error Setting 8: Small gestational age error, medium pollution exposure error;
- Error Setting 9: Small gestational age error, small pollution exposure error.

Therefore, we analyze 900 datasets in total using the newly developed model and for each model fit we collect the posterior mean estimate, 95% CI, and indicator of statistical significance (95% CI not covering zero) for each daily association parameter.

In Figure 4, we display the average posterior means and average 95% CIs across all 100 datasets for four of the error settings (1, 3, 7, 9) along with the error-free results overlaid in black (three points representing the posterior mean, lower CI limit, and upper CI limit). Results from the remaining error settings are similar and can be seen in the Supplemental Material, Figure S15. It is clear that in the case of large pollution exposure uncertainty, the posterior means are pulled towards zero as expected and the 95% CIs are longer on average. This is true regardless of the amount of gestational age error. For the remaining error settings, the estimated posterior means and CIs display a similar temporal trend to the true inference while the posterior means are generally pulled closer to zero.

In Figure 5, we display the proportion of times that each daily association parameter is identified as having a 95% CI that does not include zero for the same four error settings (post-conception pregnancy day on the x-axis). Results from the remaining error settings are similar and can be seen in the Supplemental Material, Figure S16. Recall that days 50 and 51 are identified based on the error-free inference. They are also most often identified in the simulation study results. As the amount of error decreases, particularly in pollution exposures, the probability that the correct days are identified increases overall. For high levels of error, the probability that any day has a 95% CI that doesn’t include zero is very low. This can also be seen in the average CIs of Figure 4. These results suggest that error in the estimation of gestational age and pollution exposures can mask the correct critical windows. The probability of observing a false positive is very low in each error setting and decreases as you move away from the true critical windows in each direction, with days immediately surrounding the true windows having the highest false positive rates.

These results suggest that when significant daily association parameters are identified in the actual data application, they most likely represent true critical windows or are immediately adjacent to a true critical window in the error-free inference that we are unable to observe. For very large amounts of error, particularly in the pollution exposures, the resulting inference would likely be close to null for all daily association parameters with no significant findings. Therefore, identified critical windows in our application of the model are likely not the result of misclassification error, either in gestational age or pollution concentrations. The unobserved error-free inference and our observed findings likely have similar temporal patterns in association across the pregnancy and are likely to be similar to the daily association parameters identified as significant in our application.

Discussion

We presented a new model for the identification of vulnerable daily post-conception gestational periods where increased exposure to a time-varying covariate is associated with increased association for development of specific CHDs. The general form of the model will allow different exposures to be considered. In our application, we focused on air pollution exposure in the form of $PM_{2.5}$ and showed that the model allows for the use of more detailed temporal information than the standard model, which averages the $PM_{2.5}$ exposure over post-conception gestational weeks 2–8. The standard model does not identify any statistically significant association between exposure and any of the included CHDs. However, once a finer time scale is considered, critical period associations are identified for PVS and TOF during different gestational days. These results suggest that aggregating the exposure may mask specific associations.

The cross-covariance results suggest that there is a lack of general sharing of information between the pollution parameters from different CHDs in the same broader grouping. Basing the groupings on anatomical similarities may not be informative for air pollution and birth defect epidemiology and analyzing the groupings together, as opposed to the individual defects, appears to be inappropriate. Future work could determine if alternate groupings are more informative in this setting and offer further insight into the exhibited temporal patterns. The level of similarity may also change when different time-varying exposures are considered.

Previous epidemiologic studies that only examined a single average of $PM_{2.5}$ exposure over the entire window of cardiac development did not find any elevated effect measures between pollutant exposure and individual CHDs, although two observed an inverse association between VSDs and $PM_{2.5}$ [2–4,6]. We observed some positive associations as our model allows for daily exposures across post-conception gestational weeks 2–8 while having the ability to account for the introduced multicollinearity between the exposures. Ignoring the multicollinearity by not accounting for the temporal correlation between the introduced parameters will lead to a possible lack of convergence for smaller sample sizes and increased uncertainty for the estimated parameters for larger sample sizes. Our results are similar to a previous investigation of $PM_{2.5}$ and CHDs within the NBDPS that used weekly averages to assign exposure [5]. Our examination of a finer time scale was facilitated by the use of exposure estimates from the downscaler CMAQ model, which provides daily estimates for

$PM_{2.5}$ for the entire population. This improves upon studies that utilize monitoring data, where $PM_{2.5}$ is often only measured every 3rd or 6th day and where the population is often limited to those who live within a given distance of a monitor.

Additionally, the modeling of a multinomial vector of responses allows the possibility of information sharing across the different individual defects within a broader grouping. In previous work, the amount of sharing was dictated by a fixed model parameter [5]. This model allows for more flexibility, which is important given the varying amounts of correlation within different defect-groupings. This could prove more important in different settings using other time-varying exposures. Overall, the model is shown to be flexible enough to identify individually significant associations while allowing for CHD-specific relationships with each confounder. Residual confounding is still a possibility, due both to having to collapse categories of confounders (for example combining Hispanics and Asians into an 'Other' category) to address small cell sizes and education being an imperfect measure of socioeconomic status.

The use of a finer time scale, such as the daily average exposures, could have the potential to increase exposure misclassification. Also, gestational age represents an estimate and could therefore lead to exposure misclassification when assigning daily averages of exposure. However, we do not anticipate this misclassification to vary by case-status, and thus expect that any resulting bias would be non-differential. The NBDPS collected complete residential histories during pregnancy, allowing us to avoid misclassification related to using address at delivery as well as allowing us to account for residential mobility when assigning these shorter windows of exposure. There is still the potential for misclassification due to only using home addresses, but we do not anticipate this to vary by case status. Even with potentially increased levels of misclassification, it is important to examine these finer windows of vulnerability and compare results across different methods. The consistency of our findings with similar NBDPS windows research that used weekly exposure estimates and a less complex model [5], despite having slightly different populations and exposure assessment methods, provides evidence to support our findings and suggests that our results are not due to misclassification causing an overestimation of exposure timing certainty. The presented simulation study also suggests that the resulting inference is likely similar to the error-free inference with parameter estimates closer to zero overall. We recommend similar simulation studies be carried out in future applications of the model where error amounts may differ. Using the newly developed model, we were able to identify potential daily critical windows of susceptibility to ambient $PM_{2.5}$ exposure during fetal cardiac development. This model can be applied to other time-varying exposures that may be associated with development of a selected health outcome of interest.

Supplementary Material

Refer to Web version on PubMed Central for supplementary material.

Acknowledgments

This study was supported in part through cooperative agreements under Program Announcement 02081 from the Centers for Disease Control and Prevention to the centers participating in the National Birth Defects Prevention

Study including cooperative agreement U50CCU422096. Additional support provided by the National Institute of Environmental Health Sciences (Fuentes 5R01ES014843-02, Herring R01ES020619, Herring T32ES007018).

Appendix A. Model fitting details

Use of the multinomial probit model results in semi-conjugacy in the model [28]. We fit the model using Markov chain Monte Carlo (MCMC) sampling techniques which include Gibbs sampling with a Metropolis step for selected parameters. The full conditional distribution for a single latent variable, w_{ij}, has the form of an independent truncated normal distribution with a mean of $\mathbf{x}_i^T\boldsymbol{\beta}_j+\sum_{k=k_0}^{K}\mathrm{z}\{\boldsymbol{s}_i,t_i(k)\}\eta_{g(j)}(j,k)$ and variance of one. The distribution is truncated at $\max\{\boldsymbol{w}_i(-j),0\}$ where $\boldsymbol{w}_i(-j)=(w_{i1},\ldots,w_{i,j-1},w_{i,j+1},\ldots,w_{iJ})^T$ and the direction of truncation is determined by the observed outcome. If $Y_{ij}=1$, then the distribution is strictly greater than this value, otherwise it is strictly less than this value. The w_{ij} parameters are then sampled from this truncated normal distribution one at a time where the truncation point is recalculated after each successive sample.

Next, we sample from the full conditional distribution of the $\boldsymbol{\beta}=(\boldsymbol{\beta}_1^T,\ldots,\boldsymbol{\beta}_J^T)^T$ parameter vector using Gibbs sampling once again. The $\boldsymbol{\beta}$ vector has a multivariate normal full conditional distribution with mean vector $\left\{X^TX+(\sigma_\beta^2I)^{-1}\right\}^{-1}X^T(\boldsymbol{w}-Z\boldsymbol{\eta})$ and covariance matrix $\left\{X^TX+(\sigma_\beta^2I)^{-1}\right\}^{-1}$ where $X=(X_1^T,\ldots,X_n^T)^T$ and X_i is a J by Jp block diagonal matrix with the birth i specific covariates on the diagonal, $\boldsymbol{w}=(\boldsymbol{w}_1^T,\ldots,\boldsymbol{w}_n^T)^T$, $Z=(Z_1^T,\ldots,Z_n^T)^T$ and Z_i is a J by $(J)(K+1-k_0)$ block diagonal matrix with the birth i specific daily average pollution exposures (standardized at each gestational day across all women) on the diagonal, and $\boldsymbol{\eta}=(\boldsymbol{\eta}^{(1)T},\ldots,\eta^{(G)T})^T$.

The complete $\boldsymbol{\eta}$ vector also has a convenient form useful for Gibbs sampling. The full conditional distribution has a multivariate normal form with mean vector $\left\{Z^TZ+\sum_\eta^{-1}\right\}^{-1}Z^T(\boldsymbol{w}-X\boldsymbol{\beta})$ and covariance matrix $\left\{Z^TZ+\sum_\eta^{-1}\right\}^{-1}$ where Σ_η is a block diagonal matrix with $\Omega^{(g)}\otimes\Sigma(\varphi_g)$, $g=1,\ldots,G$ on the diagonal.

The covariance matrices which control the cross covariance of the individual defects within a broader grouping also have a known full conditional form. The inverse of these matrices, $\Omega^{(g)-1}$ have a Wishart full conditional distribution with scale matrix equal to $(S+n_gI_{ng})^{-1}$ and degrees of freedom equal to $n_g+K+1-k_0$ where $S=\sum_{l=k_0}^{K}\sum_{k=k_0}^{K}\boldsymbol{\eta}_{gl}^*\boldsymbol{\eta}_{gk}^{*T}\Sigma(\phi_g)_{k,l}^{-1}$, $\boldsymbol{\eta}_{gl}^*=\{\eta_g(1,l),\ldots,\eta_g(\eta_g,l)\}^T$, and I_{ng} is the n_g by n_g identity matrix.

Finally, we update the temporal smoothness parameters (φ_g) using the Metropolis sampling algorithm. We first transform the φ_g parameters to the real line so that a normal proposal density can be used by assigning $\psi_g=\ln\left(\frac{\phi_g-a}{b-\phi_g}\right)$. Sampling is carried out for this

transformed variable and we back-transform to obtain φ_g upon completion. The log of the full conditional distribution is given as

$$-\frac{n_g}{2}\ln(|\Sigma(\phi_g)|) - \frac{1}{2}\boldsymbol{\eta}^{(g)T}\{\Omega^{(g)} \otimes \Sigma(\phi_g)\}^{-1}\boldsymbol{\eta}^{(g)} + \psi_g - 2\ln(1+\exp\{\psi_g\}).$$

References

1. van der Linde D, Konings EE, Slager MA, Witsenburg M, Helbing WA, Takkenberg JJ, et al. Birth prevalence of congenital heart disease worldwide: a systematic review and meta-analysis. Journal of the American College of Cardiology. 2011; 58:2241–2247. [PubMed: 22078432]
2. Agay-Shay K, Friger M, Linn S, Peled A, Amitai Y, Peretz C. Air pollution and congenital heart defects. Environmental Research. 2013; 124:28–34. [PubMed: 23623715]
3. Padula AM, Tager IB, Carmichael SL, Hammond SK, Yang W, Lurmann F, et al. Ambient air pollution and traffic exposures and congenital heart defects in the San Joaquin Valley of California. Paediatric and Perinatal Epidemiology. 2013; 27:329–339. [PubMed: 23772934]
4. Schembari A, Nieuwenhuijsen MJ, Salvador J, de Nazelle A, Cirach M, Dadvand P, et al. Traffic-related air pollution and congenital anomalies in Barcelona. Environmental Health Perspectives. 2013; 122:317–323. [PubMed: 24380957]
5. Stingone J, Luben T, Daniels J, Fuentes M, Richardson D, Aylsworth A, et al. Maternal exposure to criteria air pollutants and congenital heart defects in offspring: results from the National Birth Defects Prevention Study. Environmental Health Perspectives. 2014; 122:863–872. [PubMed: 24727555]
6. Vinikoor-Imler LC, Davis JA, Meyer RE, Luben TJ. Early prenatal exposure to air pollution and its associations with birth defects in a state-wide birth cohort from North Carolina. Birth Defects Research Part A: Clinical and Molecular Teratology. 2013; 97:696–701.
7. Vrijheid M, Martinez D, Manzanares S, Dadvand P, Schembari A, Rankin J, et al. Ambient air pollution and risk of congenital anomalies: a systematic review and meta-analysis. Environmental Health Perspectives. 2011; 119:598–606. [PubMed: 21131253]
8. Botto LD, Lin AE, Riehle-Colarusso T, Malik S, Correa A. Seeking causes: classifying and evaluating congenital heart defects in etiologic studies. Birth Defects Research Part A: Clinical and Molecular Teratology. 2007; 79:714–727.
9. Gittenberger-de Groot AC, Bartelings MM, Deruiter MC, Poelmann RE. Basics of cardiac development for the understanding of congenital heart malformations. Pediatric Research. 2005; 57:169–176. [PubMed: 15611355]
10. Warren J, Fuentes M, Herring A, Langlois P. Bayesian spatial-temporal model for cardiac congenital anomalies and ambient air pollution risk assessment. Environmetrics. 2012; 23:673–684. [PubMed: 23482298]
11. Berrocal VJ, Gelfand AE, Holland DM. A spatio-temporal downscaler for output from numerical models. Journal of Agricultural, Biological, and Environmental Statistics. 2010; 15:176–197.
12. Yoon PW, Rasmussen SA, Lynberg M, Moore C, Anderka M, Carmichael S, et al. The National Birth Defects Prevention Study. Public Health Reports. 2001; 116(Suppl 1):32. [PubMed: 11889273]
13. Calzolari E, Garani G, Cocchi G, Magnani C, Rivieri F, Neville A, et al. Congenital heart defects: 15 years of experience of the Emilia-Romagna Registry (Italy). European Journal of Epidemiology. 2003; 18:773–780. [PubMed: 12974553]
14. Khoury MJ, Moore CA, James LM, Cordero JF. The interaction between dysmorphology and epidemiology: methodologic issues of lumping and splitting. Teratology. 1992; 45:133–138. [PubMed: 1615423]
15. Correa A, Gilboa SM, Besser LM, Botto LD, Moore CA, Hobbs CA, et al. Diabetes mellitus and birth defects. American Journal of Obstetrics and Gynecology. 2008; 199:237.e1–237.e9. [PubMed: 18674752]

16. Warren JL, Fuentes M, Herring AH, Langlois PH. Air pollution metric analysis while determining susceptible periods of pregnancy for low birth weight. ISRN Obstetrics and Gynecology. 2013; 2013:1–9.
17. Seaman SR, Richardson S. Equivalence of prospective and retrospective models in the Bayesian analysis of case-control studies. Biometrika. 2004; 91:15–25.
18. McCulloch RE, Polson NG, Rossi PE. A Bayesian analysis of the multinomial probit model with fully identified parameters. Journal of Econometrics. 2000; 99:173–193.
19. Miller A, Riehle-Colarusso T, Siffel C, Frias JL, Correa A. Maternal age and prevalence of isolated congenital heart defects in an urban area of the United States. American Journal of Medical Genetics Part A. 2011; 155:2137–2145. [PubMed: 21815253]
20. Martin GR, Perry LW, Ferencz C. Increased prevalence of ventricular septal defect: epidemic or improved diagnosis. Pediatrics. 1989; 83:200–203. [PubMed: 2783625]
21. R Core Team. R. A Language and Environment for Statistical Computing. Vienna, Austria: R Foundation for Statistical Computing; 2013.
22. Roberts, GO. Markov chain concepts related to sampling algorithms. In: Gilks, W.; Richardson, S.; Spiegelhalter, D., editors. Markov Chain Monte Carlo in Practice. Suffolk UK: Chapman & Hall; 1996.
23. Gelman A, Rubin DB. Inference from iterative simulation using multiple sequences. Statistical Science. 1992; 7:457–472.
24. Brooks SP, Gelman A. General methods for monitoring convergence of iterative simulations. Journal of Computational and Graphical Statistics. 1998; 7:434–455.
25. Warren J, Fuentes M, Herring A, Langlois P. Spatial-temporal modeling of the association between air pollution exposure and preterm birth: identifying critical windows of exposure. Biometrics. 2012; 68:1157–1167. [PubMed: 22568640]
26. Laud PW, Ibrahim JG. Predictive model selection. Journal of the Royal Statistical Society. Series B (Methodological). 1995; 57:247–262.
27. Avery CL, Mills KT, Williams R, McGraw KA, Poole C, Smith RL, Whitsel EA. Estimating error in using ambient $PM_{2.5}$ concentrations as proxies for personal exposures: a review. Epidemiology. 2010; 21:215–223. [PubMed: 20087191]
28. Albert JH, Chib S. Bayesian analysis of binary and polychotomous response data. Journal of the American statistical Association. 1993; 88:669–679.

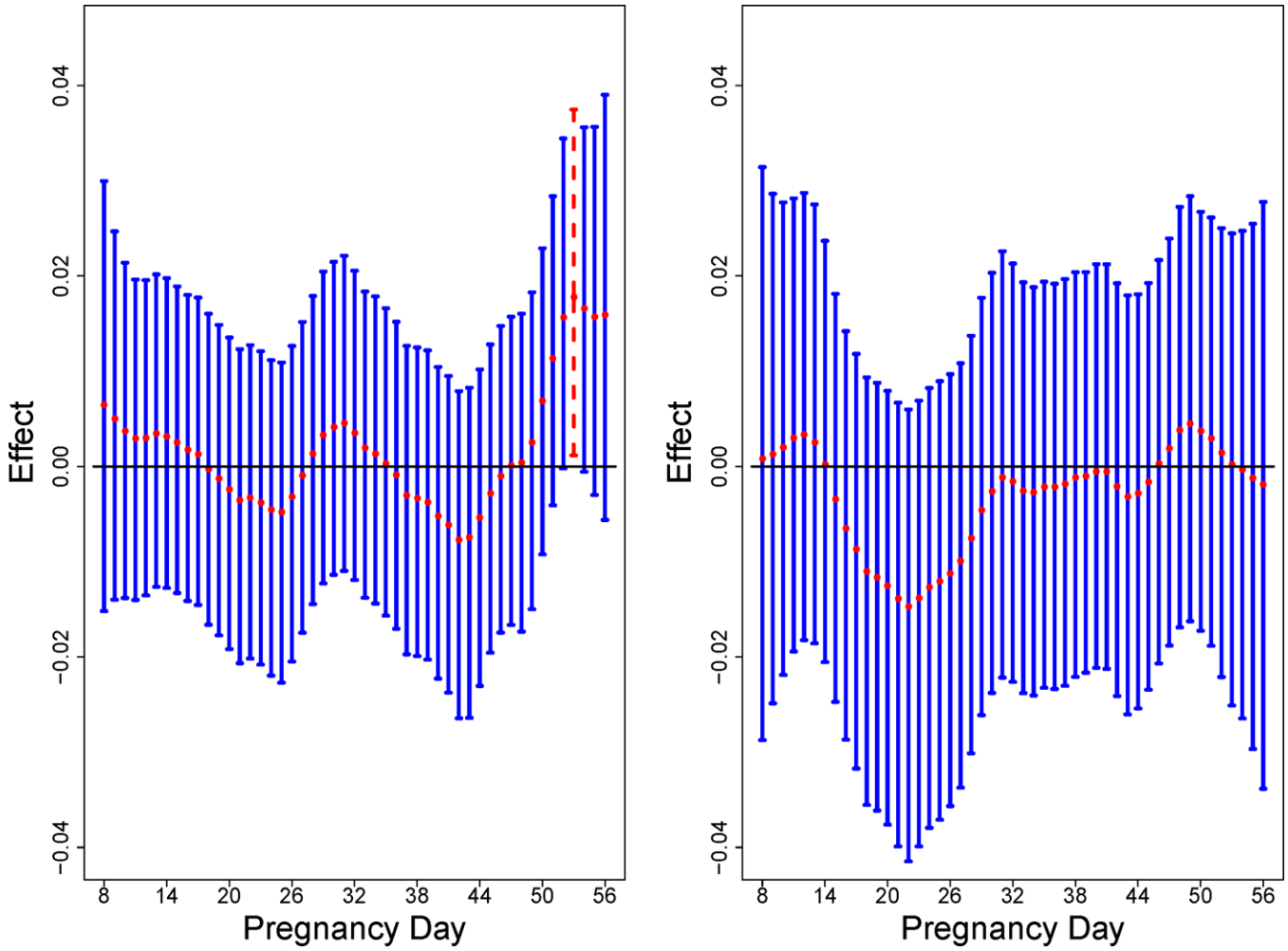

Figure 1.

Adjusted posterior means and 95% credible intervals for a change in right ventricular outflow tract obstruction defects latent variables associated with a 1-standard deviation increase in daily average $PM_{2.5}$ exposure during weeks 2 through 8 post-conception, National Birth Defects Prevention Study, 2001–2006. Individual plots correspond to (a) Pulmonary Valve Stenosis (b) Atresia. Red, dashed lines indicate that the 95% credible interval does not include zero. Adjusted for maternal race/ethnicity, maternal age, maternal education, maternal tobacco use, maternal alcohol consumption and site-specific septal case ratio.

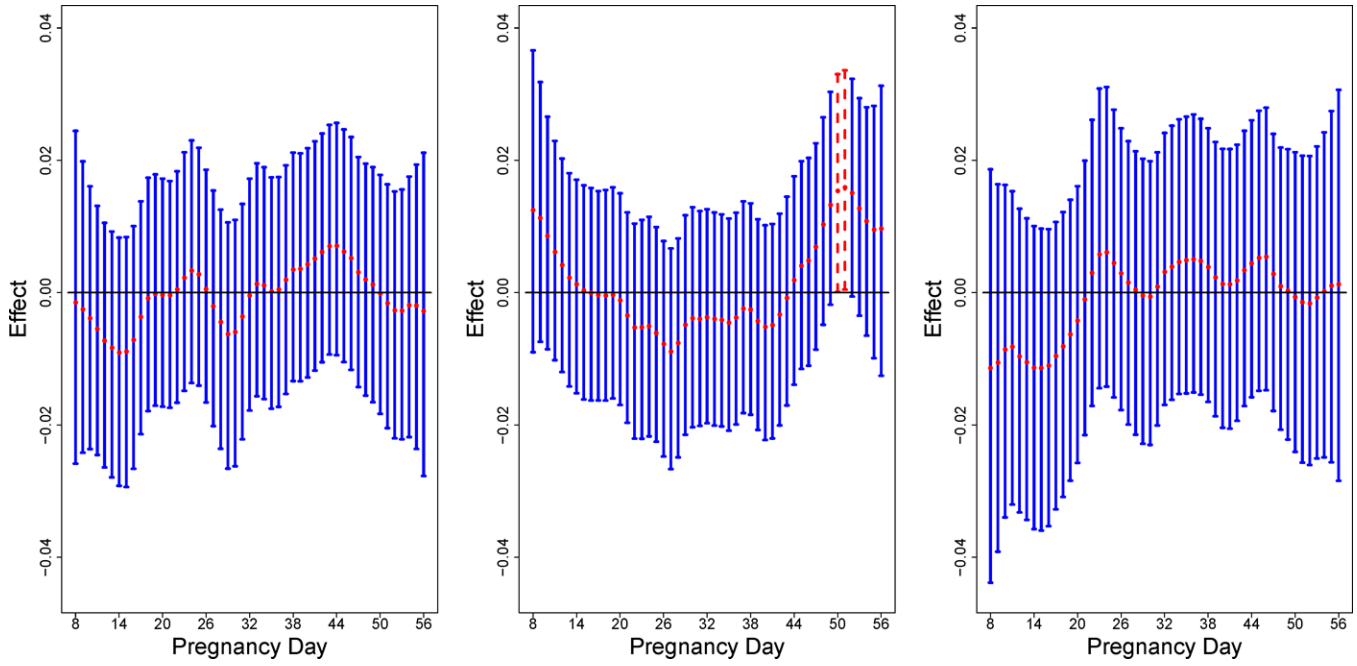

Figure 2.

Adjusted posterior means and 95% credible intervals for a change in conotruncal defects latent variables associated with a 1-standard deviation increase in daily average $PM_{2.5}$ exposure during weeks 2 through 8 post-conception, National Birth Defects Prevention Study, 2001–2006. Individual plots correspond to (a) dextro-Transposition of the Great Arteries (b) Tetralogy of Fallot (c) Other Conotruncals. Red, dashed lines indicate that the 95% credible interval does not include zero. Adjusted for maternal race/ethnicity, maternal age, maternal education, maternal tobacco use, maternal alcohol consumption and site-specific septal case ratio.

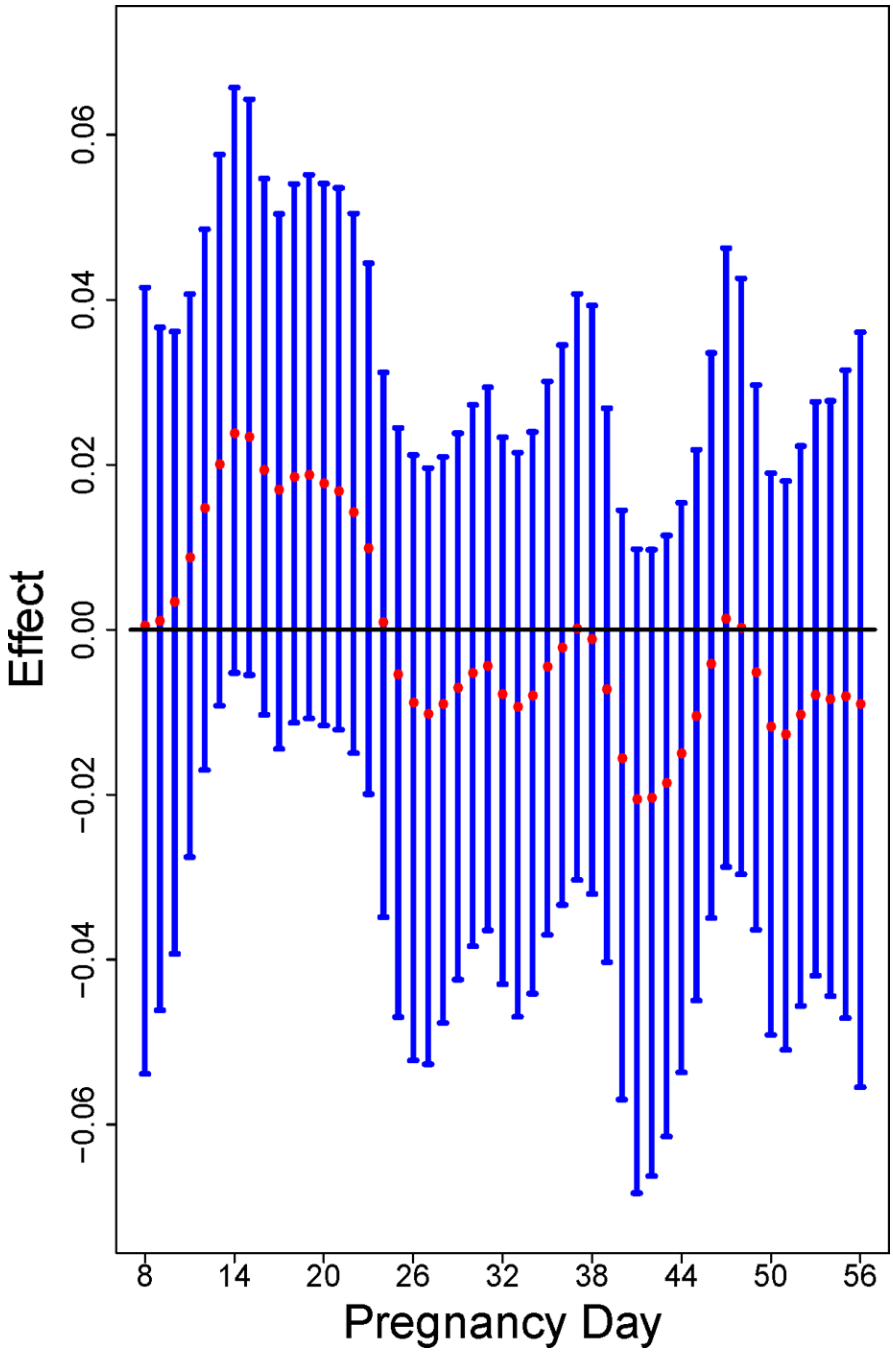

Figure 3.

Adjusted posterior means and 95% credible intervals for a change in atrioventricular septal defect latent variable associated with a 1-standard deviation increase in daily average $PM_{2.5}$ exposure during weeks 2 through 8 post-conception, National Birth Defects Prevention Study, 2001–2006. Adjusted for maternal race/ethnicity, maternal age, maternal education, maternal tobacco use, maternal alcohol consumption and site-specific septal case ratio.

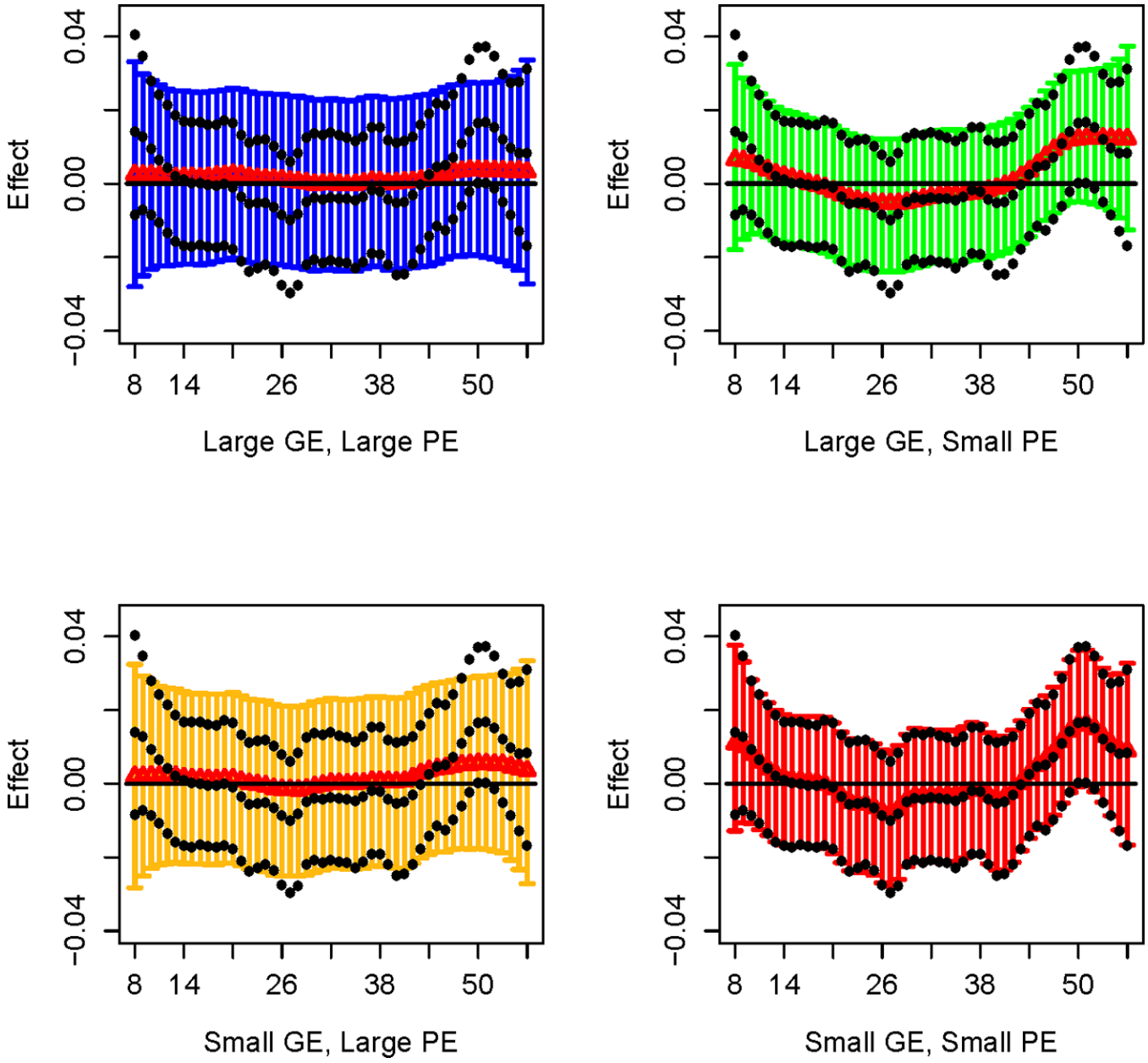

Figure 4.

Simulation study results of the average posterior means and average 95% credible intervals for four settings of gestational age error (GE) and pollution exposure error (PE). The error-free inference results are overlaid on each figure in black for comparison purposes (three points representing the posterior mean, lower CI limit, and upper CI limit). Findings from a simulated example using the Tetralogy of Fallot defect and the sample of individuals from the National Birth Defects Prevention Study, 2001–2006.

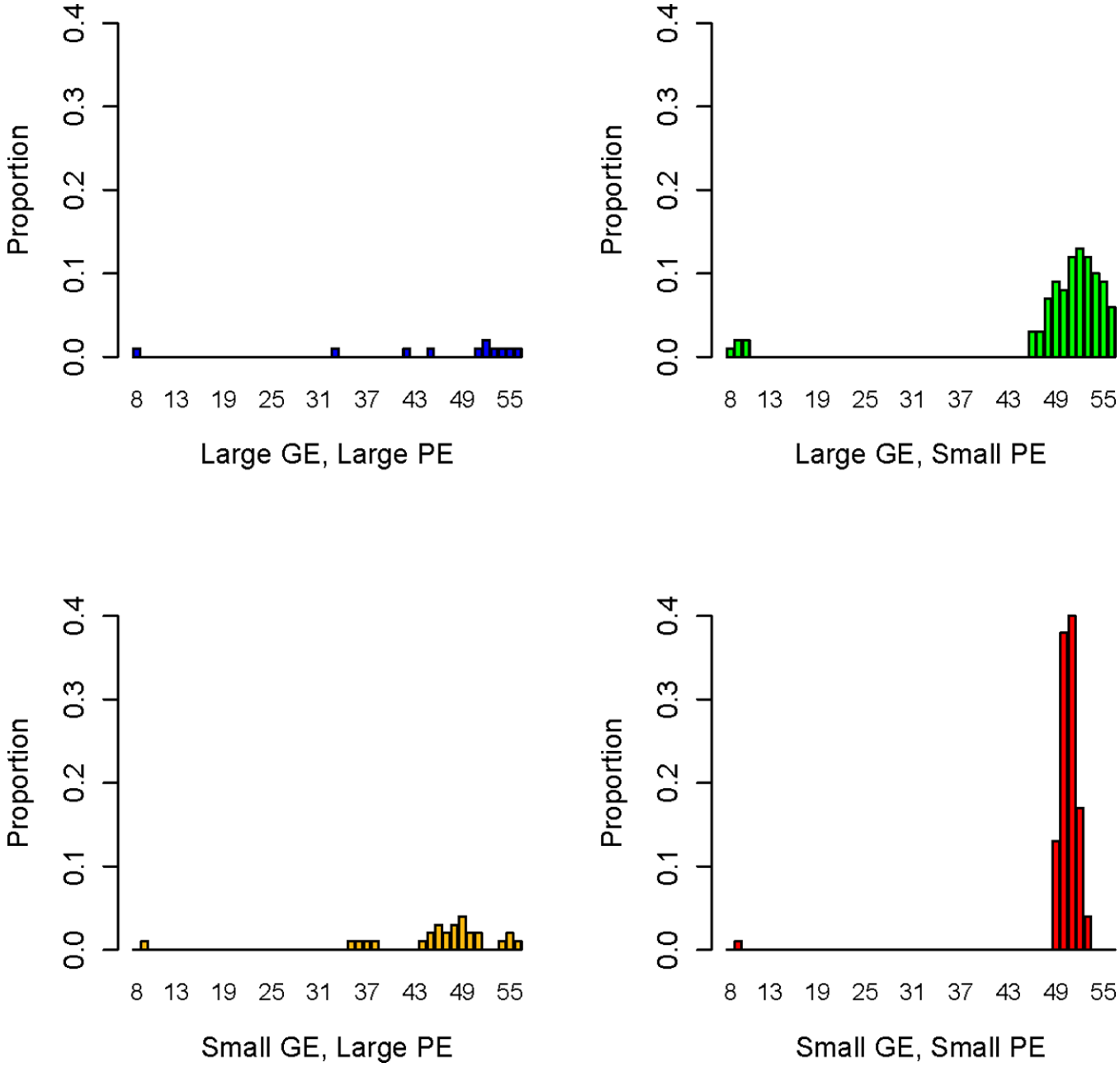

Figure 5.

Simulation study results of the proportion of times that each daily association parameter had a 95% credible interval that did not include zero for four settings of gestational age error (GE) and pollution exposure error (PE) (post-conception pregnancy day on the x-axis). Findings from a simulated example using the Tetralogy of Fallot defect and the sample of individuals from the National Birth Defects Prevention Study, 2001–2006.

Table 1

Characteristics of Congenital Heart Defect Cases and Controls in the National Birth Defects Prevention Study, 2001–2006.

Characteristic	COA	HLHS	AS	PVS	Atresia	d-TGA	TOF	OC	ASD	VSDpm	AVSD	APVR	Control
Sample Size	131	114	74	230	52	140	233	57	494	355	38	68	2741
Maternal Age (Years)													
Mean	28.95	28.11	28.85	27.61	28.85	28.62	28.90	27.19	26.52	27.97	28.42	29.04	27.65
(SD)	(5.97)	(5.89)	(5.22)	(6.10)	(6.15)	(6.32)	(6.09)	(6.04)	(6.42)	(6.58)	(5.40)	(6.19)	(6.07)
Maternal Race/Ethnicity (%)													
White/Non-Hispanic	70.99	71.05	82.43	66.52	61.54	67.86	61.80	56.14	48.38	58.87	65.79	63.24	60.12
Black/Non-Hispanic	7.63	12.28	0.00	20.00	9.62	6.43	15.02	15.79	11.54	16.62	18.42	10.29	13.72
Other	21.37	16.67	17.57	13.48	28.85	25.71	23.18	28.07	40.08	24.51	15.79	26.47	26.16
Maternal Education (%)													
< High School	16.79	15.79	4.05	14.78	15.38	11.43	10.73	19.30	22.06	17.18	7.89	16.18	15.91
High School/Some College	35.11	46.49	59.46	50.87	38.46	52.14	51.07	33.33	55.67	47.04	52.63	45.59	45.86
College/Graduate School	48.09	37.72	36.49	34.35	46.15	36.43	38.20	47.37	22.27	35.77	39.47	38.24	38.23
Smoked (First Month) (%)	12.98	12.28	18.92	19.13	15.38	15.71	15.02	15.79	22.27	16.06	23.68	16.18	15.29
Alcohol Use (First Three Months) (%)	35.88	34.21	41.89	38.70	48.08	40.71	45.92	35.09	33.40	35.21	36.84	44.12	39.15

Abbreviations: AS-aortic stenosis, APVR-anomalous pulmonary venous return, ASD-atrial septal defect, AVSD-atrioventricular septal defect, COA-coarctation of the aorta, HLHS-hypoplastic left heart syndrome, OC-other conotruncals, PVS-pulmonary vein stenosis, dTGA-dextro-transposition of the great arteries, TOF-tetralogy of Fallot, VSDpm-perimembranous ventricular septal defect.

Table 2

Adjusted Model Results Associated with an Increase of 1-Standard Deviation in 7-week Average of $PM_{2.5}$, National Birth Defects Prevention Study 2001–2006.[a]

			Quantile		
Defect	**Mean**	**SD**	**0.025**	**0.50**	**0.975**
Coarctation of the Aorta	0.05	0.04	−0.04	0.05	0.13
Hypoplastic Left Heart Syndrome	0.04	0.04	−0.05	0.04	0.13
Aortic Stenosis	−0.10	0.06	−0.21	−0.10	0.01
Pulmonary Valve Stenosis	0.04	0.04	−0.03	0.04	0.11
Atresia[b]	−0.07	0.06	−0.19	−0.07	0.05
dextro-Transposition of the Great Arteries	−0.01	0.04	−0.09	−0.01	0.07
Tetralogy of Fallot	0.03	0.03	−0.03	0.03	0.10
Other Conotruncals[c]	−0.01	0.06	−0.13	−0.01	0.10
Atrial Septal Defects	−0.03	0.03	−0.10	−0.03	0.03
Perimembranous Ventricular Septal Defects	0.00	0.03	−0.06	0.00	0.06
Atrioventricular Septal Defect	0.00	0.07	−0.13	0.00	0.13
Anomalous Pulmonary Venous Return Defects[d]	−0.05	0.06	−0.16	−0.05	0.06

Abbreviations: SD-standard deviation

[a]Model adjusted for maternal race/ethnicity, maternal age, maternal education, maternal tobacco use, maternal alcohol consumption and site-specific septal case ratio

[b]Atresia includes pulmonary and tricuspid atresia

[c]Other conotruncals include common truncus, interrupted aortic arch-type B and type not otherwise specified, double outlet right ventricle whether or not associated with transposition of the great arteries, and conoventricular septal defects

[d]Anomalous pulmonary venous return defects includes total and partial defects